LAWRENCE
LIVERMORE
NATIONAL
LABORATORY

LLNL-CONF-414924

Coherent THz electromagnetic radiation emission as a shock wave diagnostic and probe of ultrafast phase transformations

E. J. Reed, M. R. Armstrong, K. Y. Kim, J. H. Glownia, M. Howard, E. Piner, J. Roberts

July 21, 2009

APS Shock Compression of Condensed Matter
Nashville, TN, United States
June 28, 2009 through July 3, 2009

Disclaimer

Coherent THz electromagnetic radiation emission as a shock wave diagnostic and probe of ultrafast phase transformations

Evan J. Reed[*], Michael R. Armstrong[*], Ki-Yong Kim[†], James H. Glownia[†], William M. Howard[*], Edwin L. Piner[**] and John C. Roberts[**]

[*]*Lawrence Livermore National Laboratory, Livermore, CA 94551*
[†]*Los Alamos National Laboratory, Los Alamos, NM 87545*
[**]*Nitronex Corporation, Durham, NC 27703*

Abstract. We present the first experimental observations of terahertz frequency radiation emitted when a terahertz frequency acoustic wave propagates past an interface between materials of differing piezoelectric coefficients. We show that this fundamentally new phenomenon can be used to probe structural properties of thin films. Then, we present molecular dynamics simulations showing that detectable THz frequency radiation can be emitted when a wurtzite structure crystal transforms to a rocksalt structure under shock compression on picosecond timescales. We show that information about the kinetics of the transformation is contained in the time-dependence of the THz field.
Keywords: CdSe, phase transformation, shock wave, molecular dynamics, THz radiation

EXPERIMENTAL OBSERVATION WITH ACOUSTIC WAVES

As an acoustic wave traverses an interface between materials with differing piezo-electric response, polarization currents and concurrent radiation are predicted to be generated at the boundary. [1] For acoustic waves with characteristic frequencies of THz (corresponding to picosecond timescales), THz radiation is emitted. When the interface is flat and some propagation properties of the strain wave are known, the time-dependence of the strain can be computed from the time-dependence of the radiated electric field. This enables the observation of ultrafast strain profiles in regions of a material not accessible to active probes such as those used in interferometry or reflectometry based methods. Here we describe the first experimental observation of acoustically generated THz radiation that is coherently related to the strain wave time-dependence via a well-understood physical mechanism. [2] This new type of diagnostic provides information similar to a piezoelecric strain gauge but with much faster temporal response on the picosecond timescale.

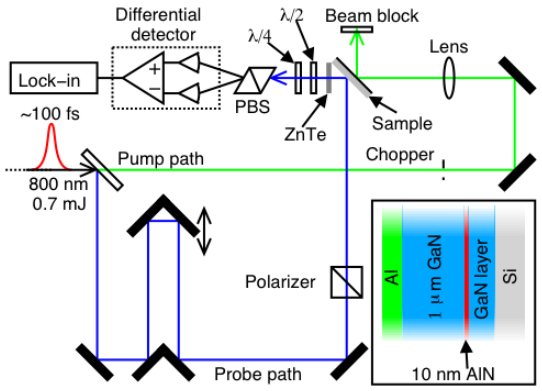

FIGURE 1. The experimental schematic. PBS is a polarizing beam separator, $\lambda/2$ and $\lambda/4$ are a half waveplate and quarter waveplate, respectively. The inset shows a cross section of the sample. The pump is incident on the Al coated side of the sample.

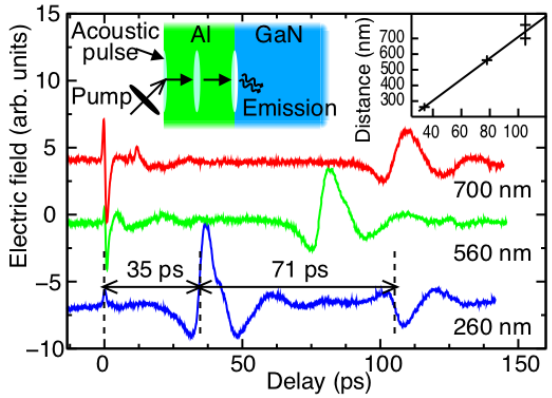

FIGURE 2. Electric field from Al/GaN interface vs. time. The plots are labeled by Al layer thickness. Dispersion in the shape of the pulse is primarily due to polycrystalline effects in the Al layer. An acoustic reflection in the Al layer radiates around 105 ps in the 260 nm Al coated sample. The transit times are labeled for the 260 nm trace. Inset: layer thickness vs. transit time in ps. A fit to the transit distance vs. time gives a sound speed of 6.7 km/s compared to the Al bulk sound speed 6.4 km/s.

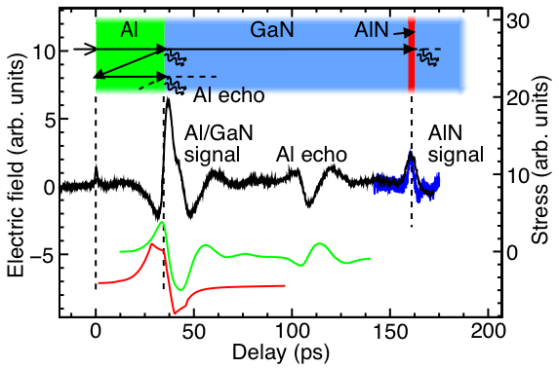

FIGURE 3. Electric field vs. time for the 260 nm Al sample (top black trace). After the stress wave initially encounters the Al/GaN interface, an acoustic echo is detected, corresponding to the acoustic wave traversing the Al layer two more times. The echo has the opposite sign compared to the initial Al/GaN signal. Signal from the AlN layer is detected at a time delay consistent with the thickness of the top GaN layer, 1 μm. Also depicted is the stress calculated from the E-field (middle green trace) compared with the stress from a simulation of the acoustic profile (red, offset from the recovered stress) having the same qualitative form.

The experimental scheme is shown in Fig. 1. In the present work, boundaries between regions of differing piezo-electric response are formed by a submicron thick layer of aluminum on gallium nitride, and a layer of AlN embedded in the GaN, as shown in the inset to Fig. 1. Piezoelectric wurtzite crystal structure GaN is oriented with its c-axis perpendicular to the sample surface. Terahertz radiation is generated when strain waves pass through the Al/GaN boundary and through the embedded AlN layer and the radiation is detected using conventional electro-optic sampling.

The acoustic wave is generated by focusing an ultrashort (100 fs) optical pulse onto the Al layer, which heats the metal within 3.5 ps through a depth of about 50 nm. Thermal expansion generates a wave with maximum strain on the order of -0.01 corresponding to pressures on the order of 1 GPa. Although the form of the acoustic wave is dependent primarily on material properties which have longer characteristic times than the pump pulse, the acoustic pulse generated at the Al surface is well synchronized with the pump.

Figure 2 shows the detected electric field for various thicknesses of Al coated on GaN. Around t=0 when the pump arrives at the Al surface, a fast THz signal is observed which is likely generated via the nonlinear optical response of the sample and/or photocurrent generation at the metal/air interface. This signal is not believed to be related to acoustic emission but provides a convenient marker for t=0. At later times, the electric field exhibits slower variation corresponding to the acoustic pulse arrival at the Al/GaN. The arrival times at the interface vary linearly with the thickness of the Al layer in each sample (cf. Figure 2 inset), demonstrating a linear correlation between the time of emission and the acoustic transit time with a fitted acoustic velocity of 6.7 km/s +/- 6% (cf. 6.4 km/s sound speed in Al). Surface probe techniques indicate that broadening of the pulse with increasing Al thickness primarily results from the distribution in sound speed as a function of grain orientation in the polycrystalline Al film.

Figure 3 shows an expanded version of data from the sample coated with 260 nm of Al along with the stress estimated from the electric field distribution via an approach related to that of Reed et al. [1, 2] This method relates the observed time-dependent electric field to the time-dependence of the stress wave at the interface. The recovered stress is qualita-

tively consistent with the expected form of an acoustic pulse excited by an ultrafast pump from a free surface. For comparison, an ALE3D simulation of the stress assuming uniform illumination at 50 mJ/cm^2 fluence is also shown. Figure 3 also shows the stress calculated from the first reflection from the Al/GaN boundary and the Al free surface, after the pulse has made two more passes through the Al layer. The reflected pulse exhibits a 180-degree total phase shift with each double pass, resulting from reflection from GaN (a higher impedance material than Al resulting in no sign change) and the free surface, which gives a 180-degree phase shift (a sign change).

PHASE TRANSFORMATION PROBE

The experiments of the previous section utilize elastic waves which do not induce plastic deformation or phase transformations in the material. In this section, we consider the nature of THz radiation emitted when plastic deformation or phase transformation occurs and what information is contained in these signals. We show that the ultrafast, shock wave induced wurtzite to rocksalt phase transformation in CdSe is accompanied by the generation of detectable THz frequency electromagnetic radiation. Motion of charged ions during transformation generates electrical currents and endows the transformed material with a static electrical polarization. This phenomenon can be thought of as an extreme nonlinear piezoelectric effect that occurs when a piezoelectric is strained to the point of phase transformation.

CdSe is a semiconducting material with applications in electronic and optical devices. Considerable interest has revolved around the synthesis and control of nanocrystalline forms. Wurtzite CdSe exhibits a high pressure transformation to the rocksalt phase which has been studied via experiments and molecular dynamics simulations in the bulk and nanocrystalline forms. The wurtzite to rocksalt transformation and its dynamical pathway have also been studied under the non-hydrostatic conditions of shock compression in CdS. [3, 4]

Figure 4 schematically shows how polarization currents can be generated when a compression wave propagates into a wurtzite structure material, or any material that lacks inversion symmetry. Figure 4(a) shows how a compression wave generated on the left

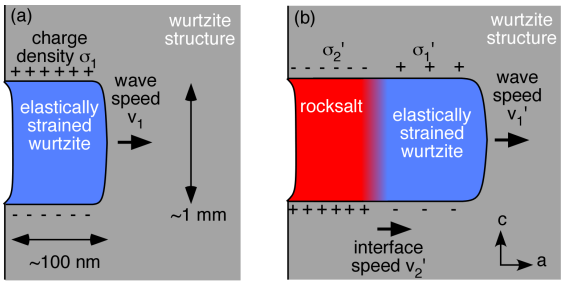

FIGURE 4. Schematic of shock waves in wurtzite generating static polarizations. (a) An elastic wave front propagates left to right with speed v_1, leaving the material behind it in a uniaxially compressed state. Static polarization charge σ_1 is generated in the c axis (vertical) direction. (b) At higher pressures, a slower wave propagates behind the elastic wave. The slower wave is associated with transformation to the rocksalt structure, exhibiting a different static polarization charge $\sigma_2' \neq \sigma_1'$.

propagating to the right generates a static polarization of the compressed material due to the piezoelectric effect. The c axis of the material is oriented in the vertical direction, leading to the production of static charge on the top and bottom of the strained region. If the charge density produced is σ_1, the polarization current per unit area generated by the shock is $j = \sigma_1 \mathrm{v}_1$ in the c lattice direction where v_1 is the propagation speed.

Figure 4(b) shows the case where the wurtzite material transforms to the rocksalt structure, accompanied by a change in static polarization. In this case, the polarization current per area is $j = \sigma_2' \mathrm{v}_2' + \sigma_1' \mathrm{v}_1'$. Depicted is the case where the elastic wave speed exceeds the speed of the transformation interface, i.e. an elastic-plastic type wave. Note that if σ_1' and σ_2' are of opposite signs, the polarization current j can potentially be of either sign. The polarization currents generate radiation which can be detected some distance away from the shock wave. Changes in the amplitude and/or sign of the radiation can indicate the onset of the phase transformation.

To explore the dynamics and fields generated by this phenomenon, we perform multi-million atom molecular dynamics simulations of shocked CdSe utilizing the LAMMPS code [5] and the CdSe potential of Rabani [6] which consists of a Coulomb interaction (effective atomic charges of magnitude 1.18) plus a Lennard-Jones interaction.

Figure 5(a) shows the magnitude of the c (unique)

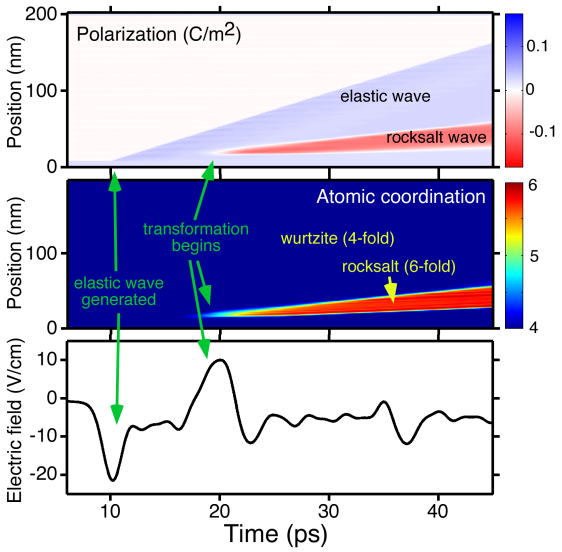

FIGURE 5. Material polarization, atomic coordination and emitted electric field for shock generated by 600 m/s piston speed. (a) An x-t diagram for the static polarization of the material in the computational cell, showing the propagation of the elastic wave (positive polarization, blue) followed by formation of rocksalt structure (negative polarization, red) around 20 ps. (b) An x-t diagram of the atomic coordination shows the coordination of most of the material is 4-fold (wurtzite) except for the rocksalt region which is 6-fold coordinated. (c) The computed electric field 2mm away shows coherent signals when the shock enters the computational cell (10 ps) and when the rocksalt transformation begins (20 ps.)

axis static polarization of the material when a shock is generated by a piston speed of 600 m/s. The uniaxial strain and stress in the shock propagation direction are -0.12 and 17 GPa respectively. The vertical axis shows distance in the shock propagation direction. The shock is generated by the piston at 10 ps. It propagates into the cell, inducing a positive change in static polarization due to the piezoelectric effect. The material is elastically strained from 10-20 ps. At 20 ps, a region of negatively polarized rocksalt begins to form near the piston and propagates away more slowly than the elastic wave. Figure 5(b) shows the coordination of the material. The material is all 4-fold coordinated (wurtzite) except for the formation of 6-fold coordinated rocksalt beginning around 20 ps. Figure 5(c) shows the time-dependence of the electric field generated by the polarization currents in the simulation for a typical experimental configuration. We have previously developed a technique for calculating the electromagnetic radiation from a molecular dynamics simulation. [7] The peak at 10 ps corresponds to the shock entering the CdSe. Such signals were initially predicted by our earlier work [1] and subsequently experimentally observed in the previous section. [2] A feature around 20 ps indicates the onset of the rocksalt phase transformation. This feature has sign opposite to the 10 ps feature because the polarization of the rocksalt material is opposite in sign to the elastically compressed wurtzite, shown in Figure 5(a). Observation of the delay between these pulses provides information about the kinetics of the transformation.

ACKNOWLEDGMENTS

We thank R. Averitt, C. Bolme, P. Celliers, R. Chau, R. Collins, J. Eggert, L. Fried, D. Funk, D. Hicks, N. Holmes, A. Lindenberg, D. Moore, J. Nguyen, R. Patterson, and C. Tarver for helpful discussions. This work was supported by the LLNL LDRD program, the LANL CINT user program, and performed in part under the auspices of the U.S. Department of Energy by Lawrence Livermore National Laboratory under Contract DE-AC52-07NA27344.

REFERENCES

1. Reed, E. J., Armstrong, M. R., Kim, K., and Glownia, J. H., *Phys. Rev. Lett.*, **101**, 014302 (2008).
2. Armstrong, M. R., Reed, E. J., Kim, K.-Y., Glownia, J. H., Howard, W. M., Piner, E. L., and Roberts, J. C., *Nature Physics*, **5**, 285 (2009).
3. Sharma, S. M., and Gupta, Y. M., *Phys. Rev. B*, **58**, 5964 (1998).
4. Knudson, M. D., Gupta, Y. M., and Kunz, A. B., *Phys. Rev. B*, **59**, 11704 (1999).
5. Plimpton, S. J., *J. Comp. Phys.*, **117**, 1 (1995).
6. Rabani, E., *J. Chem. Phys.*, **116**, 258 (2002).
7. Reed, E. J., Soljačić, M., Gee, R., and Joannopoulos, J. D., *Phys. Rev. Lett.*, **96**, 013904 (2006).